Published in final edited form as:

Curr Biol. 2021 July 12; 31(13): 2887–2894.e4. doi:10.1016/j.cub.2021.04.018.

Rab34 is necessary for early stages of intracellular ciliogenesis

Michael W. Stuck[1], **Weng Man Chong**[2], **Jung-Chi Liao**[2], **Gregory J. Pazour**[1,‡]

[1]Program in Molecular Medicine, University of Massachusetts Medical School, Biotech II, Suite 213, 373 Plantation Street, Worcester, MA 01605

[2]Institute of Atomic and Molecular Sciences, Academia Sinica, Taipei, 10617, Taiwan

Summary

Primary cilia are sensory organelles present on most vertebrate cells and are critical for development and health. Ciliary dysfunction is associated with a large class of human pathologies collectively known as ciliopathies. These include cystic kidneys, blindness, obesity, skeletal malformations and other organ anomalies. Using a proximity biotinylation with Ift27 as bait, we identified the small GTPase Rab34 as a ciliary protein. Rab34 localizes to the centrosomes near the mother centriole, the axoneme of developed cilia, and highly dynamic tubule structures in the centrosomal region. Rab34 is required for cilia formation in fibroblasts, where we find that Rab34 loss blocks ciliogenesis at an early step of ciliary vesicle formation. In IMCD3 epithelial cells, the requirement is more complex with Rab34 needed in cells grown at low density but becoming less important as cell density increases. Ciliogenesis can proceed by an internal pathway where cilia form in the cytoplasm before being displayed on the ciliary surface or cilia can assemble by an external pathway where the centriole docks on the plasma membrane before ciliary assembly. Fibroblasts are thought to use the internal pathway, while IMCD3 cells are thought to use the external pathway. However, we find that IMCD3 cells can use the internal assembly pathway and significant numbers of internally assembling cilia are observed in low-density cells. Together our work indicates that Rab34 is required for internal assembly of cilia but not for cilia built on the cell surface.

eTOC:

Stuck et al. show that Rab34 is required for the formation of the ciliary vesicle at the initiation of intracellular ciliogenesis. Rab34 is dispensable in IMCD3 epithelial cells that utilize the

‡Corresponding Author: Lead Contact, Telephone: 508 856 8078, gregory.pazour@umassmed.edu, Twitter: @greg_pazour.

Author Contributions

Conceptualization: M.W.S. and G.J.P.
Methodology: M.W.S., W.M.C., J.-C.L. and G.J.P.
Investigation: M.W.S., W.M.C. and J.-C.L.
Writing – Original Draft: M.W.S. and G.J.P.
Writing – Review and Editing: M.W.S., W.M.C., J.-C.L. and G.J.P.
Supervision: J.-C.L. and G.J.P.
Funding Acquisition: J.-C.L. and G.J.P.

Declaration of Interests

The authors declare no competing interests

extracellular ciliogenesis pathway when grown at high density, but is important when cells are grown at a low density that promotes intracellular assembly.

Keywords

intraflagellar transport; Hedgehog signaling; cilia; smoothened

Results and Discussion

Ift27-BirA labels a subset of ciliary proteins.

Most types of eukaryotic cilia are built and maintained by intraflagellar transport (IFT). Our previous work indicated that the IFT-B subunit Ift27 is a critical interface between IFT and ciliary signaling but details are lacking [1–4]. To gain information on Ift27 function, we used proximity biotinylation to identify proteins located near Ift27. An Ift27-BirA* fusion protein expressed in *Ift27*$^{-/-}$ mouse embryonic fibroblasts (MEFs) [2, 5] biotinylates cilia (Figure 1A) and complements a Smo trafficking defect in these cells (Figure 1B). Purification of biotinylated proteins shows that Ift25, the direct binding partner of Ift27, and Ift81, a component of IFT-B are biotinylated in cells expressing Ift27-BirA* but not in controls (Figure 1C). Combined, this data shows that our Ift27-BirA* construct is functionally incorporated into the IFT-B complex and is able to biotinylate ciliary proteins.

To identify Ift27 interacting proteins, we scaled up the purification and subjected the biotinylated proteins to mass spectrometry. Five independent Ift27-BirA* and five control preparations were analyzed. Using iBAQ quantification, 119 proteins were enriched more than 10 fold in the experimental samples relative to the controls (Table S1). Importantly, this included the 10 IFT-B core subunits but no peripheral IFT-B subunits and no components of IFT-A or the BBSome (Figure 1D). Finding IFT-B core subunits without other components of the IFT complex highlights the specificity of this approach and suggests that the collection of biotinylated proteins contains Ift27 neighbors and is likely to identify new proteins important for ciliary assembly or function.

Rab34 is a ciliary protein.

Focusing on proteins that could have a regulatory role, we noted that Rab34 is enriched 13 fold by Ift27-BirA* compared to the controls. Interestingly, *Rab34*$^{-/-}$ mice share cleft palate, polydactyly, micrognathia, and preweaning lethality with *Ift27*$^{-/-}$ mutant mice (https://www.mousephenotype.org/data/genes/MGI:104606) [2, 6]. Rab34 is a small GTPase found exclusively in metazoans [7, 8]. Originally, it was found to localize to the Golgi complex and regulate lysosome position [8] through interactions with the Rab-interacting lysosomal protein, Rilp. Rab34 also interacts with the Rilp-related proteins, Rilpl1 and Rilp2 that localize to cilia and centrosomes, and regulate ciliary composition [9, 10]. While this project was underway, independent work demonstrated that Rab34 localizes to cilia and is required for ciliogenesis [6, 11].

Using Flag-tagged Rab34, we confirmed the Golgi, cilia and centrosome localization of Rab34 (Figures 1E, S1A, S1B, and S2A). Using an antibody against the endogenous protein,

we found that Rab34 localizes to a small percentage of cilia (8.3+/− 4.4%) of cilia (Figure 1F) where it co localizes with Ift27 (Figure 1G). We are not able to detect Golgi localization of endogenous Rab34 with any staining method (Figure S1A), suggesting that the Golgi localization is an artifact of over expression or the amount of native protein at the Golgi complex is below our detection limit. The presumptive GTP-locked (Q111L) form of Rab34 localized like wild type to the cilium and the Golgi complex while the presumptive nucleotide-free or GDP-locked (T66N) mutant was dispersed in the cell with no enrichment at any organelle (Figure S2A).

To determine if Rab34 and Ift27 directly interact, we immunoprecipitated Rab34 from control and *Ift27*$^{-/-}$ cells. Rab34 was detected in both precipitates, but Ift27 was not detected (Figure S1C) suggesting that Rab34 and Ift27 are not physically associated or if they are, the binding strength is not strong enough to withstand the procedure. In addition, we did not observe any alteration of Rab34 localization when Ift27 was missing (Figure S1B).

Rab34 is required for ciliogenesis.

Rab34 is only found in a low percentage of cilia in serum-starved populations. Rab8 shows similar behavior due to its transient association with cilia only during assembly [12]. To determine if Rab34 localization to cilia varied by state of assembly, we fixed cells before serum starvation and at intervals after ciliary assembly was initiated. This revealed a variety of Rab34 localization patterns that we classified into six groups (Figure 2A). Class 0 cells lacked an axoneme (as detected by acetyl-alpha tubulin stain) and did not show Rab34 enrichment near the centrosome. Class 1 cells lacked an axoneme but the centrosome was positive for Rab34. Class 2 cells lacked an axoneme but had Rab34-positive tubules projecting from the centrosome. Class 3 cells had an axoneme along with Rab34-positive tubules projecting from the base and/or the tip of the cilium. Class 4 cells had a Rab34-positive cilium but had no associated tubules. Class 5 cells were ciliated but were negative for Rab34.

To determine if the classes of Rab34 localization represent states of ciliary assembly, we quantitated the distribution of cells in these six groups prior to ciliary assembly (not serum starved), after 3 hrs of serum starvation to interrogate early stages of ciliogenesis and after 48 hrs to observe patterns when ciliogenesis is largely concluded (Figure 2A). Prior to serum starvation and at three hrs post starvation, most cells (<60%) showed enrichment of Rab34 at the centrosome (class 1) and by 48 hrs most cells (68%) were ciliated and lacked Rab34 label. Rab34-positive tubules projecting from a non-ciliated centrosome (class 3) was highest at the 3 hr time point and Rab34-positive cilia (class 4 and 5) was highest at 48 hrs. This distribution supports a model where Rab34 is involved in ciliary assembly, but is not needed for ciliary maintenance.

Our results show that prior to serum starvation, most cells have Rab34 localized to a spot near the centrosome. In cells with duplicated and separated centrosomes, Rab34 colocalizes with Cep164 indicating that it is associated with mature centrioles with distal appendages (Figure 2B). Distal appendages are assembled in an ordered process that starts with Cep83 recruiting Sclt1 and Cep89. Sclt1 then recruits Cep164, which in turn recruits Ttbk2. To determine where in this process Rab34 acts, we used CRISPR/Cas9 to target genes encoding

distal appendage proteins to create non-clonal KO cell lines and quantified how this affected Rab34 to recruitment to the centrosome prior to ciliogenesis (Figure 2C). Loss of Cep89 did not affect the recruitment of Rab34. However, guides against the Sclt1/Cep164/Ttbk2 branch reduced the recruitment of Rab34 indicating that it is likely recruited to the centrosome through this complex. Airy scan confocal microscopy shows that Rab34 localizes to small puncta that are distal to the Cep164 ring (Figures 2D and 2E). It is likely that these puncta represent pre-ciliary vesicles docked at the distal appendages prior to ciliary assembly.

During ciliary assembly, we noted that Rab34 localized to small tubules that projected from the centrosome or cilium (Figure 2A, class 2). Similar tubules were observed when assembling cilia were stained for Rab8, pacsin-2 and Ehd1 [13]. To determine if the Rab34-positive tubules are the same as observed by Insinna, we co-stained MEFs for Rab34 and either Rab8 or pacsin-2. While Rab34, Rab8, and pacsin-2 all label the same tubular network, we found a surprising amount of diversity in the colocalization patterns. We observed tubules positive for both Rab8 and Rab34 along with tubules positive for Rab34 but lacking Rab8 and ones positive for Rab8 but missing Rab34 (Figure 2F). Similarly, when we compare Rab34 with pacsin-2, we find tubules that show colocalization as well as pacsin-2-positive tubules that lack Rab34 and ones positive for Rab34 but lack pacsin-2 (Figure 2G).

Rab34 label of class 3 and 4 cilia often gave the appearance of being slightly different from the ciliary marker Arl13b. To explore this further, we used dSTORM to image cilia that were positive for Rab34 (Figure S2B). Arl13b label was on average 198 nm wide, which was significantly narrower than Rab34 label at 282 nm (Figure S2C). Arl13b is a myristoylated peripheral membrane protein and is thought to label the ciliary membrane. Rab34 is predicted to be a prenylated peripheral membrane protein. If Rab34 also localized to the ciliary membrane, we would expect it to show a similar diameter as Arl13b but the larger diameter suggests that Rab34 is labeling a membrane surrounding the cilium such as the ciliary pocket membrane or an extension of the outer membrane of the ciliary vesicle.

A known Rab34 binding partner, Rilpl1, was previously connected to cilia and proposed to act as a regulator of ciliary membrane protein levels [9, 10]. Interestingly when we examined the localization of Rab34 and Rilpl1, we found that unlike Rab8 and Pacsin-2, Rab34 and Rilpl1 always co-localized (Figure 3A). dSTORM analysis confirmed extensive colocalization of Rab34 and Rilpl1 and showed that the width of their labels are similar (Figure 3B) suggesting that Rab34 and Rilpl1 are localized to the same membrane. The heterogeneity of Rab34, Rab8, pacsin-2, and Rilpl1 localization to ciliary vesicle-associated tubules suggests these structures are more complicated than previous appreciated and mechanisms exist to sort proteins to tubule subdomains.

To determine the importance of Rab34 to ciliogenesis, we used CRISPR/Cas9 to knockout Rab34 from MEFs. Two independent guide RNAs were generated and transfected into cells. The resulting mixed populations were sorted by flow cytometry to generate clonal lines that were screened by western blot (Figure S3A). Interestingly, cells lacking Rab34 assembled almost no cilia (Figure S3B). The ciliogenesis phenotype was rescued by re-expression of Flag-Rab34 or GTP-locked Flag-Rab34^{Q111L} but not by nucleotide-free or GDP-locked

Flag-Rab34^{T66N} or by Flag-Rab34$^{C257A/C258A}$, a mutant where the C-terminal prenylation motif was mutated (Figure S3B).

The ciliary and centrosomal localization of Rilpl1 was lost in *Rab34*$^{-/-}$ cells and this was not rescued by transfection with Flag-Rab34 (Figure S3C and S3D). To explore this finding further, we compared rescue with untagged Rab34 to Flag-Rab34. Both constructs rescued ciliation to a similar extent (Figures S3C and S3E), but only the untagged Rab34 restored Rilpl1 to cilia (Figures S3C and S3D). Previous work suggested that the loss of Rilpl1 increases ciliary Smo levels at the basal state [10]. However, we did not detect a significant difference in Hedgehog signaling in cells rescued with Flag-Rab34 compared to those rescued with untagged Rab34 (Figure S3F). Thus, the recruitment of Rilpl1 to cilia by Rab34 is not essential for cilia formation or Hedgehog signaling although we cannot rule out subtle effects undetected by our analysis.

The presence of Rab34 in a subset of cilia after 48 hrs of serum starvation (Figure 2A, class 4) raises the question of whether this represents ciliary turnover or whether Rab34 transiently associates with cilia after assembly. To test these possibilities we wanted to follow Rab34 localization by live cell imaging. Our observation that N-terminally tagged Rab34 failed to rescue the Rilpl1 phenotype raised questions about whether an N-terminal fusion of a fluorescent protein onto Rab34 would give legitimate results. The C-terminus of Rab34 cannot be tagged as this would disrupt the prenylation site that is required for activity (Figure S3B). Since disruption of Rilpl1 had little effect on the cell and Rilpl1 is tightly colocalized with Rab34, we imaged Rilpl1 as a surrogate for Rab34. Imaging cells expressing mCherry-Rilpl1 and eGFP-Ccsap (to mark the cilium and centrosome [14]) showed that mCherry-Rilpl1 transiently associated with assembled cilia (Figure 3C, Video S1 and S2). The first movie illustrates the mobility of the tubules, which are constantly changing size and position. The second movie illustrates the dynamic nature of the association of Ripl1 with cilia. In this example, at time 0 the cilium is positive for Rilpl1, Rilpl1 signal is lost after 190 seconds of observation and returns at time 410. Taken together these results are consistent with Rab34 being transiently recruited to the ciliary pocket of mature cilia, although this method does not distinguish if these are external cilia or internal cilia prior to emergence.

To determine where in the intracellular ciliogenesis pathway Rab34 is acting, we determined how its loss affects the localization of critical components during ciliary assembly. Internal ciliogenesis begins with the recruitment of Rab11-positive vesicles to the centrosome by the TRAPPII complex with assistance from myosin5a and pacsin-2. Rab11 then brings rabin8 into contact with Rab8 to initiate formation of the ciliary membrane [12, 13, 15, 16]. Upon serum starvation, GFP-Rab11 colocalized to a tight focus at the centrosome with Rab34, likely the ciliary vesicle, but in the mutant cells GFP-Rab11 remained in a peri-centrosomal localization (Figure 4A). Consistent with the failure to organize the Rab11-positive vesicles, Rab8, myosin5a and pacsin-2, which are thought to act downstream of Rab11 failed to accumulate on ciliary vesicle tubules at the centrosomes of *Rab34*$^{-/-}$ cells and this localization was restored in rescue cells (Figure 4B). In agreement with published work [6], we found that *Rab34*$^{-/-}$ cells were able to remove CP110 similar to controls (WT: 88.2% +/− 6.7; *Rab34*$^{-/-}$: 93.4% +/− 2.0 have removed CP110 from one centriole, not significantly

different). Our data supports a model in which Rab34 plays a role in coordinating the formation of the ciliary vesicle and associated tubules after the delivery of the early ciliary proteins to the region of the centrosome. Independent analysis of myosin5a and Rab8 indicates that the effects of Rab34 on their local concentration might vary from cell type to cell type but defects in ciliary vesicle formation are universally observed [6, 17]. IFT-B proteins are found at centrosomes regardless of whether ciliary assembly is occurring or not [18, 19]. This localization appears to be independent of Rab34, as we detected no changes to the distribution of the IFT-A component Ift140 and the IFT-B component Ift27 when Rab34 is missing (Figure 4C).

Mice lacking cilia typically show more severe phenotypes [20] than observed in the *Rab34* mutant mouse, which is inconsistent with our observation that loss of Rab34 blocked ciliogenesis in MEFs. One possible explanation for this discrepancy is that Rab34's role in ciliogenesis is cell type specific. To test this possibility we knocked out Rab34 in inner medullary collecting duct (IMCD3) cells, which are epithelial in contrast to the MEFs that are mesenchymal. *Rab34*$^{-/-}$ IMCD3 cells plated at high density and serum starved showed normal levels of ciliation. However, we noted that these cells plated at low cell density were poorly ciliated. To test the link between cell density and ciliogenesis in these cells, we plated serial dilutions of control and *Rab34*$^{-/-}$ IMCD3 cells, and quantitated the ability of these cells to produce cilia at each density (Figure 4D). At high densities, differences in ciliation are small but as the cells become less dense, the impact of Rab34 on ciliation becomes apparent.

Ciliary assembly in IMCD3s involves migration of the centriole to the cell surface before extension of the axonemal microtubules (extracellular assembly) whereas the process in MEFs starts in the cytoplasm with the formation of a ciliary vesicle (intracellular pathway). Our findings suggest that Rab34 is needed for the intracellular ciliogenesis pathway but not for the extracellular pathway. To further test this idea we used an IN/OUT assay [21] to track the presence of internal, partially exposed, and totally exposed cilia in WT and *Rab34*$^{-/-}$ IMCD3 cells (Figure 4E). With decreasing cell density, the percentage of internal or partially exposed cilia increases in WT supporting the idea that IMCD3 cells can utilize the internal assembly pathway at low cell density. In contrast, *Rab34*$^{-/-}$ cells have fewer internal and partially exposed cilia than control and the percentage does not change with cell density. The reduced number of internal and partially exposed cilia in the mutant supports a role for Rab34 in internal assembly but also indicates that IMCD3 cells have a mechanism to bypass the need for Rab34 for internal assembly. However, we cannot rule out the possibility that partially exposed cilia could result from retraction of surface assembled cilia. Our finding that Rab34 is particularly important for internal assembly is consistent with published work showing Rab34 is required for ciliogenesis in hTERT-RPE1, NIH-3T3 and MCF10 cells but not in MDCK cells [6, 11, 22]. Ciliary assembly in MCF10 cells has not been explored, but hTERT-RPE1 and NIH3T3 cells are thought to use the intracellular pathway while MDCK cells are thought to use the extracellular pathway. The relatively subtle phenotype of the Rab34 knockout mouse compared to animals completely lacking cilia is consistent with cilia defects being found in only a subset of cells in the animal. In the *Rab34* knockout mouse, cilia were reduced in the limb bud and neural tube [6]. Tissue-specific loss of cilia also was observed in mice lacking proteins of the tectonic complex [23]. Interestingly, there is an

inverse relationship to the affected cells in the tectonic mutants compared to the Rab34 mutants. For example, tectonic-1 mutants form cilia in the limb bud while these are missing in Rab34 mutants. Tectonic-1 mutants lack cilia on the node and show left-right patterning defects while Rab34 mutant show normal left-right patterning suggesting these cilia are intact. Rab34 mutant fibroblasts lack cilia while tectonic-1 mutant fibroblasts can form cilia to some extent. The tectonic proteins are components of the ciliary transition zone, a structure at the base of all cilia. The observation that the tectonic proteins are less important in cells that require Rab34 for assembly suggests that the transition zone is more important to extracellular assembly than it is for intracellular assembly. Perhaps the membrane cytoskeletal linkage provided by the transition zone is critical to the docking of the centriole on the cell surface but not as important for the initial steps of ciliary vesicle formation in the cytoplasm.

In summary, our work indicates that Rab34 is required for the early steps of ciliogenesis by the intracellular assembly pathway but is dispensable for ciliary assembly by the extracellular pathway.

STAR Methods

Resource Availability

Lead contact—Further information and requests for resources and reagents should be directed to and will be fulfilled by the lead contact, Gregory Pazour (gregory.pazour@umassmed.edu).

Materials Availability—Cell lines, plasmids, and other reagents generated in this study are available upon request. Plasmids will be deposited in Addgene.

Data and code availability—The published article includes all datasets generated or analyzed during this study (Table S1).

Experimental Model and Subject Details

Cell Culture—Wild type and *Ift27*$^{-/-}$ mouse embryonic fibroblasts (MEFs) were derived from E14 embryos and immortalized with SV40 Large T antigen [2]. Cell lines were authenticated by genotyping the *Ift27* locus. *Rab34*$^{-/-}$, *Cep83*$^{-/-}$, *Sclt1*$^{-/-}$, *Cep89*$^{-/-}$, *Cep164*$^{-/-}$, *and Ttbk2*$^{-/-}$ cells were obtained by genome editing of immortalized wild type MEFs using guides cloned into pLentiCRISPRv2 (Addgene plasmid # 52961) and confirmed by western blot or PCR amplification of the genomic DNA followed by Sanger sequencing [24]. All MEFs were cultured in 95% DMEM (4.5 g/L glucose), 5% fetal bovine serum, 100 U/ml penicillin, and 100 microgram/ml streptomycin (all from Gibco-Invitrogen).

IMCD3 cells [25] were cultured in 47.5% DMEM (4.5 g/L glucose), 47.5% F12, 5% fetal bovine serum, 100 U/ml penicillin, and 100 microgram/ml streptomycin (all from Gibco-Invitrogen).

For smoothened agonist (SAG) experiments, MEFs were plated at near confluent densities and serum starved (same culture medium described above but with 0.25% FBS) for 48 hr to allow ciliation. SAG (Calbiochem) was added to the serum starve media at 400 nM for the last 24 hr prior to harvest.

Method Details

Plasmids—Plasmids were assembled by Gibson assembly (NEB, Ipswitch MA) into the pHAGE lentiviral backbone [26]. All inserts are derived from mouse unless otherwise stated. All inserts were fully sequenced and matched NCBI reference sequence or expected mutant forms. SnapGene files will be provided upon request.

Lentivirus Production—Lentiviral packaged pHAGE-derived plasmids [26] were used for transfection. These vectors were packaged by a third-generation system comprising four distinct packaging vectors (Tat, Rev, Gag/Pol, and VSV-g) using HEK 293T cells as the host. DNA (Backbone: 5 μg; Tat: 0.5 μg; Rev: 0.5 μg; Gag/Pol: 0.5 μg; VSV-g/: 1 μg) was delivered to the HEK cells using calcium phosphate precipitation. After 48 hrs, supernatant was harvested, filtered through a 0.45-micron filter and added to subconfluent cells. After 24 hrs, cells were selected with puromycin (Puro, 1 microgram/ml) or blasticidin (Bsd, 60 micrograms/ml).

Immunofluorescence—Cells were fixed with 2% paraformaldehyde for 15 min, permeabilized with 0.1% Triton-X-100 for 2 min and stained as described [18]. In some cases, fixed cells were treated with 0.05% SDS for 5 min before prehybridization to retrieve antigens.

Widefield images were captured using an Orca ER or an FLIR camera on a Zeiss Axiovert 200M microscope equipped with a 100x Zeiss objective (Thornwood, NY). Contrast adjustment and cropping was done in ImageJ or Photoshop.

For dSTORM imaging, detailed procedures and instrument setup were as previously described [27]. Briefly, cells were grown on coverslips; Alexa Fluor 647 antibody (1:200) and Cy3B-conjugated antibody (1:100) were used as secondary antibodies. During imaging, the coverslip was immersed in imaging buffer which included TN buffer at pH 8.0, and an oxygen-scavenging system consisting of 60–100 mM mercaptoethylamine (MEA, 30070, Sigma-Aldrich) at pH 8.0, 0.5 mg/mL glucose oxidase (G2133, Sigma-Aldrich), 40 mg/mL catalase (C40, Sigma-Aldrich), and 10% (w/v) glucose (G8270, Sigma-Aldrich). The 647 nm and 561 nm laser lines were operated at a high intensity of ~1–5 kW/cm2 consecutively to acquire corresponding signals. Images were analyzed by ImageJ.

Live cell images were captured using an Andor iXon^{EM+} 885K camera, with binning set to 2, on an Olympus ix71 Microscope equipped with a 60x Olympus objective (1.49NA) with the 1.6x optivar in place (Center Valley, PA). Excitation light was provided by 491nm and 561nm Cobalt Lasers (HÜBNER Photonics, San Jose, CA). Emission light was filtered by 525/50 and 605/50 bandpass filters (Chroma Technology, Bellow Falls, VT). Images were captured at 0.1Hz with a 50ms Exposure. Focus stabilization was controlled by pgFocus (Biomedical Imaging Group, http://big.umassmed.edu/wiki/index.php/PgFocus).

Confocal images were captured on a Zeiss LSM 900 + Airyscan microscope using a Plan Apo 63x (Zeiss) objective and controlled by Zen 3.1 blue Zeiss) software.

For the IN/OUT assay, WT and *Rab34*$^{-/-}$ IMCD3 cells expressing SmoM2-GFP (GFP was inserted between amino acids 32 and 33 in the extra cellular N-terminal tail of SmoM2) were grown in medium with 5% FBS. Exposed GFP was labeled by first fixing the cells using 4% paraformaldehyde in PBS followed by blocking with 5% BSA in PBS and labeling with an anti-GFP antibody (3E6, Invitrogen). Following this step, cover slips were washed, briefly fixed again to lock the GFP antibody in place, cells then were permeabilized with 0.1% Triton-X-100 in PBS and stained with a second anti-GFP antibody (DSHB-GFP-12A6, DSHB) and rabbit Arl13b to mark cilia. Images were captured on a Zeiss LSM 900 + Airyscan microscope using a Plan Apo 63x (Zeiss) objective and controlled by Zen Blue 3.1 (Zeiss) software.

Protein and mRNA Analysis—For western blots, MEFs were lysed directly into denaturing gel loading buffer (Tris-HCl 125 mM pH6.8, glycerol 20% v/v, SDS 4% v/v, β-mercaptoethanol 10% v/v, bromophenol blue). Western blots were developed by chemiluminescence (Super Signal West Dura, Pierce Thermo) and imaged using an Amersham Imager 600 or Biorad ChemiDoc XRS+.

For biotin pulldown, cells were serum starved for 48 hrs in 0.25% FBS DMEM + 50uM Biotin and proteins were extracted with RIPA buffer (1% TX-100, 0.5% Sodium Deoxycholate, 50mM Tris-HCl, pH 7.5, 150mM NaCl, 1mM EDTA, 1mM EGTA, 0.1% SDS) with protease inhibitor (Complete EDTA-Free, Roche). Insoluble components were removed by centrifugation at 20000g. Cell extract was pre-cleared before addition to a 50% slurry of Thermo High Capacity NeutrAvidin Resin (Thermo Scientific, 29202) and incubated overnight with gentle agitation 4°C. Beads were washed 5X with RIPA buffer before elution at 65°C for 10 min with elution buffer (30mM Biotin, 2% SDS, 50mM Tris pH 7.4, 10mM EDTA). Gel loading buffer was added to the eluates for SDS-PAGE electrophoresis and Western blotting analysis.

The list of candidate proteins was generated using Scaffold (Proteome Software Inc., version 4.8.8,) by averaging the IBAQ values from five Ift27 experimental and five control samples, replacing 0 and −1 values with 1 and then calculating the ratio of experimental/control. Proteins were considered candidates if they were at least 10 fold enriched in Ift27, at least 1/100 as abundant as Ift27, present in at least three experimental samples but not present in more than two control samples.

Isolation of mRNA and quantitative mRNA analysis was performed as previously described [28].

Quantification and Statistical Analysis

Samples used to generate data in Figures 2A, 2C, 4D, 4E, S3B, S3D and S3E were blinded to the observer. Data groups were analyzed by as described in the figure legends using GraphPad Prism (San Diego CA). Differences between groups were considered statistically

significant if $p < 0.05$. Statistical significance is denoted with asterisks (*p=0.01 – 0.05; **p=0.01–0.001; ***p<0.001–0.0001, ****p<0.0001). Error bars are all S.D.

Supplementary Material

Refer to Web version on PubMed Central for supplementary material.

Acknowledgments

We thank Dr. Carol E. Schrader and the staff of the UMMS Flow Cytometry Core and Karl Bellve of the UMMS Biomedical Imaging Group for assistance during this project. This work was supported by the National Institutes of Health GM060992 and DK103632 to GJP.

Abbreviations:

IFT	intraflagellar transport
MEFs	mouse embryonic fibroblasts
SAG	smoothened agonist
WT	wild type

References

1. Wang Z, Fan ZC, Williamson SM, and Qin H (2009). Intraflagellar transport (IFT) protein IFT25 is a phosphoprotein component of IFT complex B and physically interacts with IFT27 in Chlamydomonas. PLoS One 4, e5384. [PubMed: 19412537]
2. Eguether T, San Agustin JT, Keady BT, Jonassen JA, Liang Y, Francis R, Tobita K, Johnson CA, Abdelhamed ZA, Lo CW, et al. (2014). IFT27 links the BBSome to IFT for maintenance of the ciliary signaling compartment. Dev Cell 31, 279–290. [PubMed: 25446516]
3. Liew GM, Ye F, Nager AR, Murphy JP, Lee JS, Aguiar M, Breslow DK, Gygi SP, and Nachury MV (2014). The intraflagellar transport protein IFT27 promotes BBSome exit from cilia through the GTPase ARL6/BBS3. Dev Cell 31, 265–278. [PubMed: 25443296]
4. Keady BT, Samtani R, Tobita K, Tsuchya M, San Agustin JT, Follit JA, Jonassen JA, Subramanian R, Lo CW, and Pazour GJ (2012). IFT25 links the signal-dependent movement of Hedgehog components to intraflagellar transport. Dev Cell 22, 940–951. [PubMed: 22595669]
5. Kim DI, Jensen SC, Noble KA, Kc B, Roux KH, Motamedchaboki K, and Roux KJ (2016). An improved smaller biotin ligase for BioID proximity labeling. Mol Biol Cell 27, 1188–1196. [PubMed: 26912792]
6. Xu S, Liu Y, Meng Q, and Wang B (2018). Rab34 small GTPase is required for Hedgehog signaling and an early step of ciliary vesicle formation in mouse. J Cell Sci 131.
7. Morimoto BH, Chuang CC, and Koshland DE Jr. (1991). Molecular cloning of a member of a new class of low-molecular-weight GTP-binding proteins. Genes Dev 5, 2386–2391. [PubMed: 1752434]
8. Wang T, and Hong W (2002). Interorganellar regulation of lysosome positioning by the Golgi apparatus through Rab34 interaction with Rab-interacting lysosomal protein. Mol Biol Cell 13, 4317–4332. [PubMed: 12475955]
9. Wang T, Wong KK, and Hong W (2004). A unique region of RILP distinguishes it from its related proteins in its regulation of lysosomal morphology and interaction with Rab7 and Rab34. Mol Biol Cell 15, 815–826. [PubMed: 14668488]
10. Schaub JR, and Stearns T (2013). The Rilp-like proteins Rilpl1 and Rilpl2 regulate ciliary membrane content. Mol Biol Cell 24, 453–464. [PubMed: 23264467]

11. Oguchi ME, Okuyama K, Homma Y, and Fukuda M (2020). A comprehensive analysis of Rab GTPases reveals a role for Rab34 in serum starvation-induced primary ciliogenesis. J Biol Chem 295, 12674–12685. [PubMed: 32669361]
12. Westlake CJ, Baye LM, Nachury MV, Wright KJ, Ervin KE, Phu L, Chalouni C, Beck JS, Kirkpatrick DS, Slusarski DC, et al. (2011). Primary cilia membrane assembly is initiated by Rab11 and transport protein particle II (TRAPPII) complex-dependent trafficking of Rabin8 to the centrosome. Proc Natl Acad Sci U S A 108, 2759–2764. [PubMed: 21273506]
13. Insinna C, Lu Q, Teixeira I, Harned A, Semler EM, Stauffer J, Magidson V, Tiwari A, Kenworthy AK, Narayan K, et al. (2019). Investigation of F-BAR domain PACSIN proteins uncovers membrane tubulation function in cilia assembly and transport. Nat Commun 10, 428. [PubMed: 30683896]
14. Backer CB, Gutzman JH, Pearson CG, and Cheeseman IM (2012). CSAP localizes to polyglutamylated microtubules and promotes proper cilia function and zebrafish development. Mol Biol Cell 23, 2122–2130. [PubMed: 22493317]
15. Lu Q, Insinna C, Ott C, Stauffer J, Pintado PA, Rahajeng J, Baxa U, Walia V, Cuenca A, Hwang YS, et al. (2015). Early steps in primary cilium assembly require EHD1/EHD3-dependent ciliary vesicle formation. Nat Cell Biol 17, 228–240. [PubMed: 25686250]
16. Nachury MV, Loktev AV, Zhang Q, Westlake CJ, Peranen J, Merdes A, Slusarski DC, Scheller RH, Bazan JF, Sheffield VC, et al. (2007). A core complex of BBS proteins cooperates with the GTPase Rab8 to promote ciliary membrane biogenesis. Cell 129, 1201–1213. [PubMed: 17574030]
17. Ganga AK, Kennedy MC, Oguchi ME, Gray SD, Oliver KE, Knight TA, De La Cruz EM, Homma Y, Fukuda M, and Breslow DK (2020). Rab34 GTPase mediates ciliary membrane biogenesis in the intracellular ciliogenesis pathway. bioRxiv.
18. Follit JA, Tuft RA, Fogarty KE, and Pazour GJ (2006). The intraflagellar transport protein IFT20 is associated with the Golgi complex and is required for cilia assembly. Mol Biol Cell 17, 3781–3792. [PubMed: 16775004]
19. Delaval B, Bright A, Lawson ND, and Doxsey S (2011). The cilia protein IFT88 is required for spindle orientation in mitosis. Nat Cell Biol 13, 461–468. [PubMed: 21441926]
20. Murcia NS, Richards WG, Yoder BK, Mucenski ML, Dunlap JR, and Woychik RP (2000). The Oak Ridge Polycystic Kidney (orpk) disease gene is required for left-right axis determination. Development 127, 2347–2355. [PubMed: 10804177]
21. Kukic I, Rivera-Molina F, and Toomre D (2016). The IN/OUT assay: a new tool to study ciliogenesis. Cilia 5, 23. [PubMed: 27493724]
22. Ganga AK, Kennedy MC, Oguchi ME, Gray SD, Oliver KE, Knight TA, De La Cruz EM, Homma Y, Fukuda M, and Breslow DK (2020). Rab34 GTPase mediates ciliary membrane biogenesis in the intracellular ciliogenesis pathway. bioRxiv, 2020.2010.2029.360891.
23. Garcia-Gonzalo FR, Corbit KC, Sirerol-Piquer MS, Ramaswami G, Otto EA, Noriega TR, Seol AD, Robinson JF, Bennett CL, Josifova DJ, et al. (2011). A transition zone complex regulates mammalian ciliogenesis and ciliary membrane composition. Nat Genet 43, 776–784. [PubMed: 21725307]
24. Sanjana NE, Shalem O, and Zhang F (2014). Improved vectors and genome-wide libraries for CRISPR screening. Nat Methods 11, 783–784. [PubMed: 25075903]
25. Rauchman MI, Nigam SK, Delpire E, and Gullans SR (1993). An osmotically tolerant inner medullary collecting duct cell line from an SV40 transgenic mouse. Am J Physiol 265, F416–424. [PubMed: 8214101]
26. Wilson AA, Kwok LW, Hovav AH, Ohle SJ, Little FF, Fine A, and Kotton DN (2008). Sustained expression of alpha1-antitrypsin after transplantation of manipulated hematopoietic stem cells. Am J Respir Cell Mol Biol 39, 133–141. [PubMed: 18323534]
27. Chong WM, Wang WJ, Lo CH, Chiu TY, Chang TJ, Liu YP, Tanos B, Mazo G, Tsou MB, Jane WN, et al. (2020). Super-resolution microscopy reveals coupling between mammalian centriole subdistal appendages and distal appendages. Elife 9.

28. Jonassen JA, San Agustin J, Follit JA, and Pazour GJ (2008). Deletion of IFT20 in the mouse kidney causes misorientation of the mitotic spindle and cystic kidney disease. J Cell Biol 183, 377–384. [PubMed: 18981227]

29. Pazour GJ, Baker SA, Deane JA, Cole DG, Dickert BL, Rosenbaum JL, et al. (2002). The intraflagellar transport protein, IFT88, is essential for vertebrate photoreceptor assembly and maintenance. J. Cell Biol 2002; 157, 103–113 [PubMed: 11916979]

30. Jonassen JA, SanAgustin J, Baker SP, Pazour GJ (2012). Disruption of IFT complex A causes cystic kidneys without mitotic spindle misorientation. J. Am. Soc. Nephrol 2012; 23, 641–651 [PubMed: 22282595]

Highlights:

- Proximity biotinylation with Ift27-BirA identified Rab34 as a ciliary protein.
- Rab34 is required for ciliogenesis in fibroblasts.
- Rab34 is needed for an early step of ciliary vesicle formation.
- The importance of Rab34 in IMCD3 ciliogenesis decreases with increasing cell density.

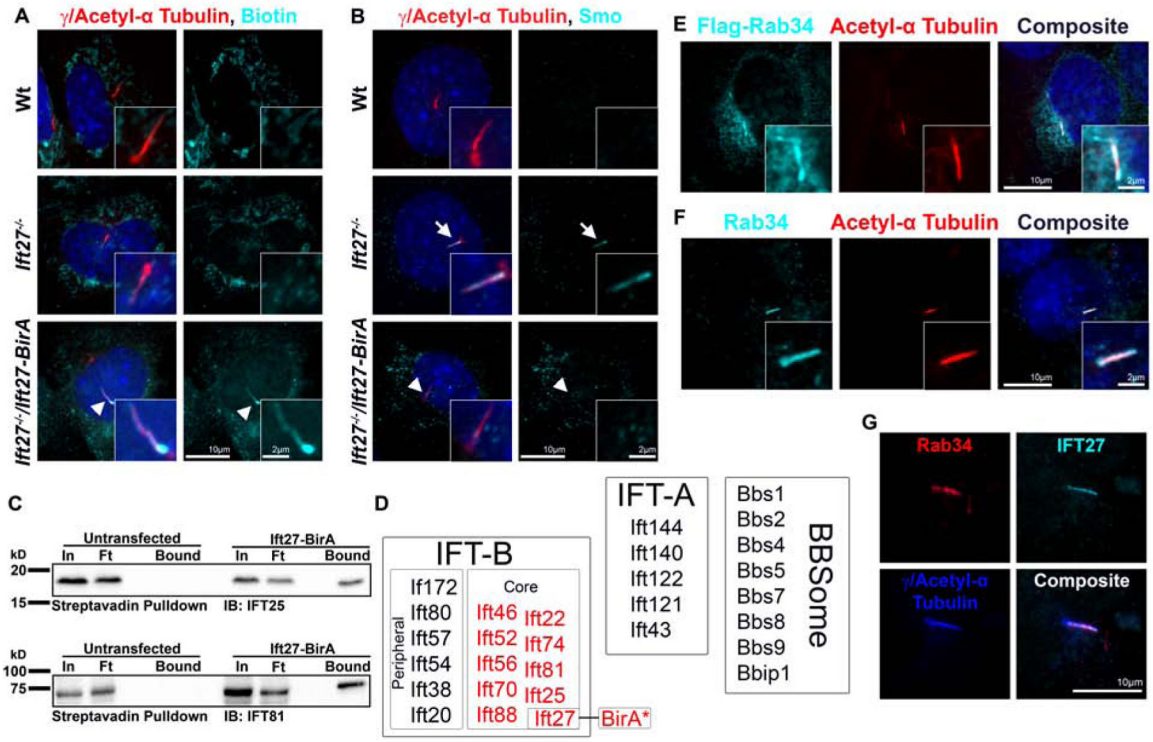

Figure 1. Ift27-BirA labels ciliary proteins including Rab34.

(A) Wild type, *Ift27*$^{-/-}$, and *Ift27*$^{-/-}$/Ift27-BirA* MEFs stained for cilia/centrosomes (gamma and acetyl-alpha tubulin, red) and biotinylated proteins (cyan). *Ift27*$^{-/-}$/Ift27-BirA* cilia are enriched in biotinylated proteins (arrowhead). Insets are 2x enlargements. Scale bars are 10 and 2 microns for the main images and insets respectively.

(B) Smoothened (cyan) abnormally accumulates (arrow) in *Ift27*$^{-/-}$ cilia (red) while this trafficking defect is rescued by the expression of Ift27-BirA* (arrowhead). Scale bars are 10 and 2 microns for the main images and insets respectively.

(C) Biotinylated IFT-B components, Ift25 (top) and Ift81 (bottom), were pulled down using streptavidin conjugated beads from Ift27-BirA expressing cells but not from controls. In=Input, Ft=Flow Through.

(D) Diagram of IFT-A, IFT-B and BBSome complex subunits with positive hits indicated (red).

(E) Flag-Rab34 (cyan) localizes to MEF cilia (red) when overexpressed. Insets are 2x enlargements. Scale bars are 10 and 2 microns for the main images and insets respectively.

(F) Endogenous Rab34 (cyan) localizes to MEF cilia (red). Insets are 2x enlargements. Scale bars are 10 and 2 microns for the main images and insets respectively.

(G) Endogenous Rab34 (red) localizes with Ift27 (cyan) to cilia (blue) in a subset of WT cilia. Scale bar is 10 microns.

See also Table S1 and Figure S1.

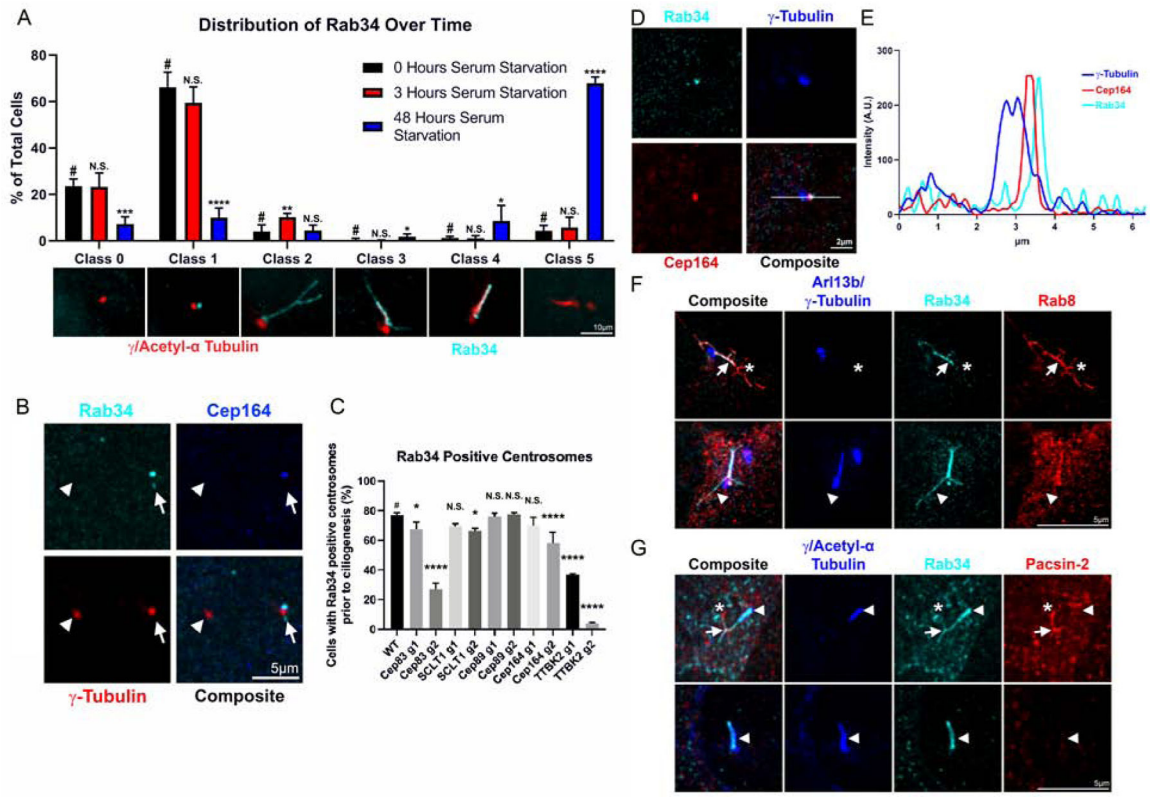

Figure 2. Rab34 localizes to the ciliary vesicle and ciliary pocket membranes and is dynamic during ciliogenesis.

(A) In MEF cells, Rab34 (endogenous protein, cyan) localization relative to cilia/centrosomes (gamma and acetyl-alpha tubulin, red) can be classified into distinct patterns (examples below) that change over time (quantified above). n=129 cells counted from 3 independent experiments. Statistical comparisons are within each class as compared to 0 hours (#).

(B) In MEF cells, Rab34 (cyan, arrow) localizes to mother centrioles labeled by gamma tubulin (red) and Cep164 (blue) but is absent from daughter centrioles labeled by gamma tubulin alone (arrowhead). Scale bar is 5 microns.

(C) The importance of distal appendage proteins to Rab34 recruitment was assessed by transfecting WT MEF cells with two independent guides targeting distal appendage genes and counting Rab34 positive centrosomes prior to ciliogenesis. n=>100 cells from 3 independent replicates analyzed by one-way ANOVA compared to control (#).

(D) Airy scan confocal microscopy shows that Rab34 (endogenous protein, cyan) localizes distal relative to gamma tubulin (blue) and Cep164 (red) in MEF cells. Scale bar is 2 microns. The line marks the scan shown in E.

(E) Line analysis of signal intensity from composite image in D.

(F-G) In MEF cells, Rab34 (endogenous protein, cyan) positive membrane tubules are also positive for Rab8 (red, F) and pacsin-2 (red, G) although distinct regions show Rab34 and Rab8/pacsin-2 colocalization (arrows), Rab34 alone (arrowhead) and Rab8/pacsin-2 alone (*). Cilia are blue. Two examples are shown. Scale bars are 5 microns.

See also Figure S2.

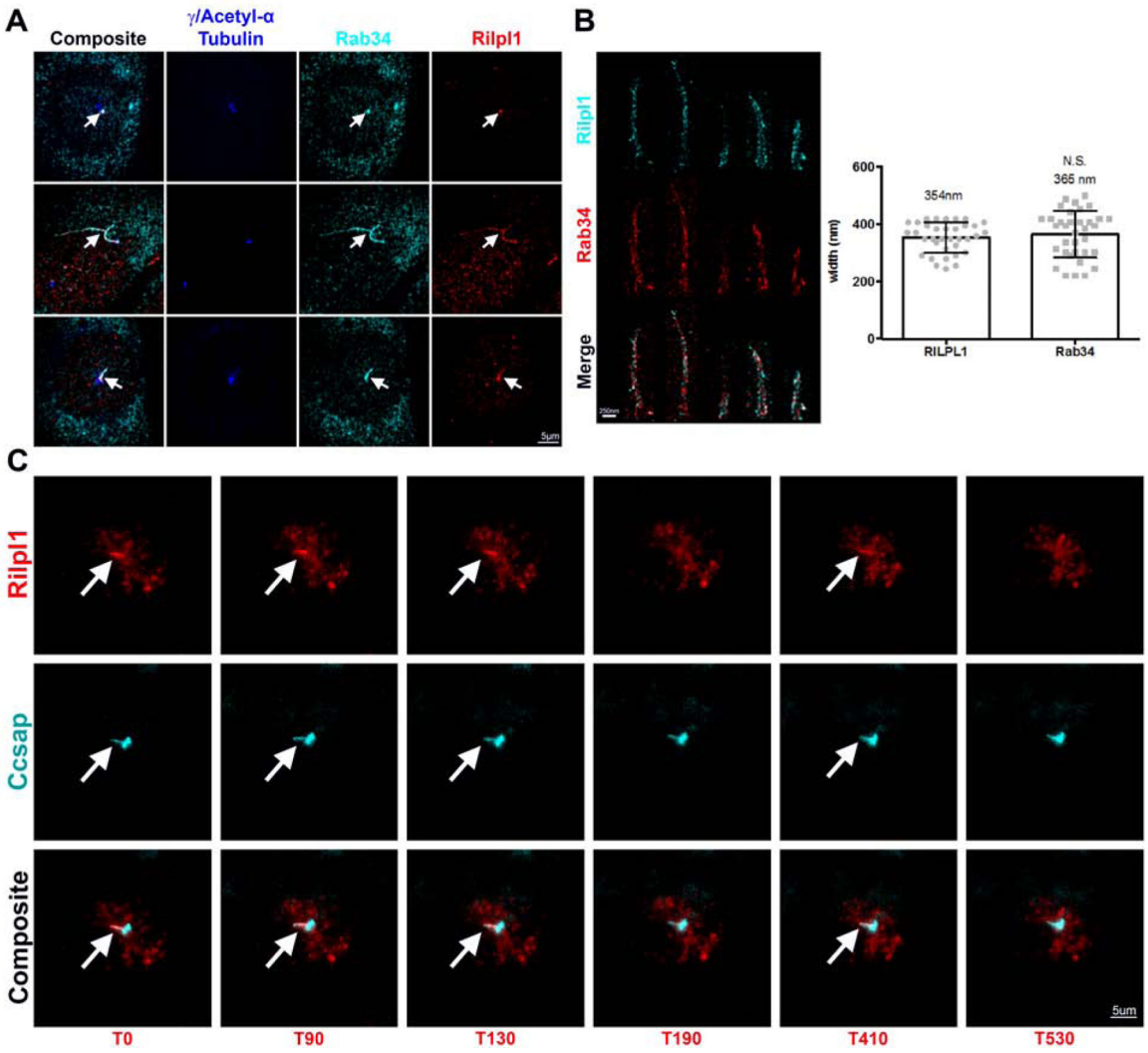

Figure 3. Rilpl1 localization indicates dynamic trafficking to mature cilia.

(A) Rab34 (endogenous protein, cyan) and Rilpl1 (red) co-localize (arrow) at the centrosome (top), on membrane tubules (middle) and at the cilia (bottom) in MEF cells. Cilia/centrosomes (blue) were labeled using a mix of acetyl-alpha tubulin and gamma tubulin antibodies. Scale bar is 5 microns.

(B) Rilpl1 (cyan) and Rab34 (red) localization in MEF cells was examined by dSTORM (left). The width of Rilp1 and Rab34 label in the bottom 0.8 microns was quantified (right). Scale bar is 250nm.

(C) Selected images from Video S2. Localization of mCherry-Rilpl1 (red) to the cilium (arrow) is dynamic in MEF cells. Cilia are marked by eGFP-Ccsap (cyan). Time from initial image is indicated in seconds.

See also Video S1, Video S2, and Figure S3.

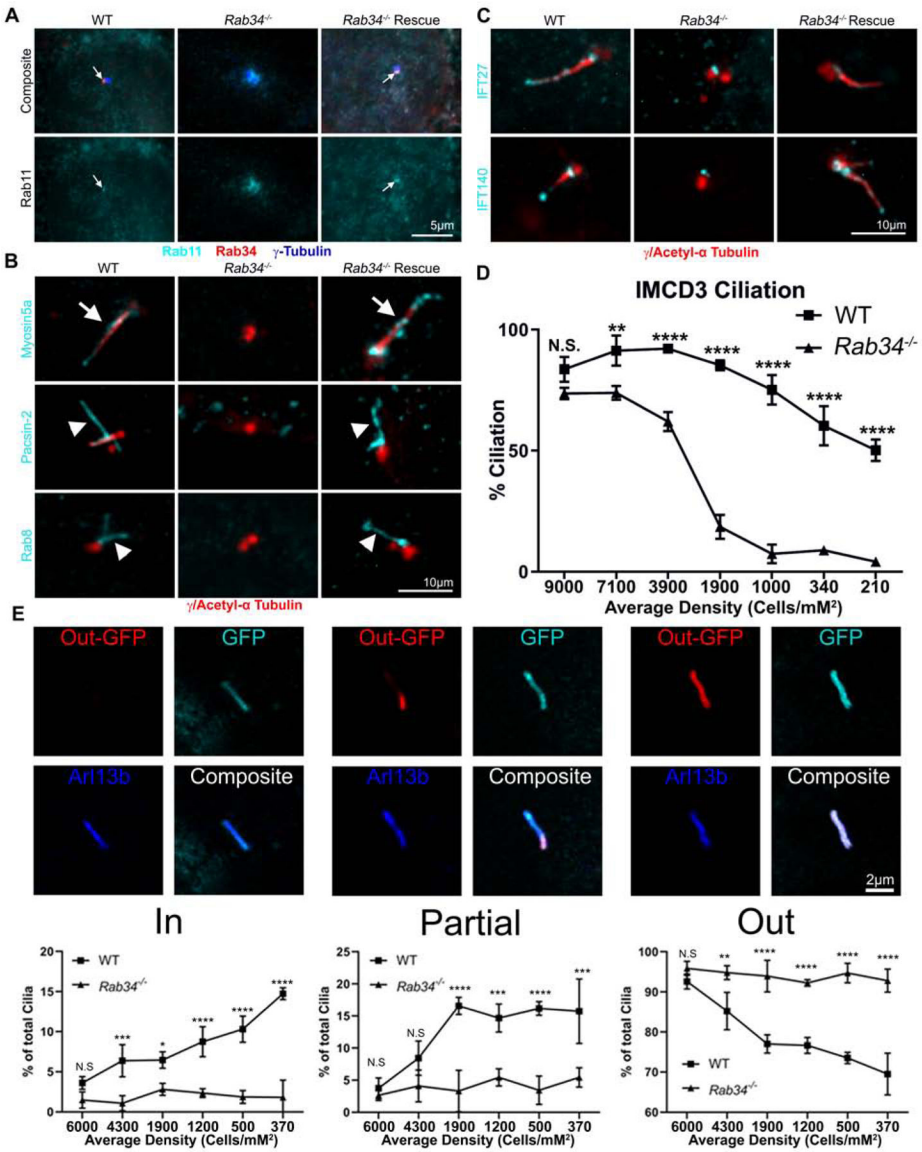

Figure 4. Rab34 is necessary for early stages of ciliogenesis

(A) GFP-Rab11 (cyan) localizes to the peri-centriolar region in the WT, *Rab34*$^{-/-}$, and *Rab34*$^{-/-}$ rescue MEF cells. Rab34 (endogenous protein, red) and GFP-Rab11 co-localize (arrows) in WT and rescue cells. Scale bar is 5 microns.

(B) The recruitment of the early ciliogenesis proteins myosin5a (cyan, top), pacsin-2 (green, middle), and Rab8 (cyan, bottom) to the developing cilia in MEFs is disrupted in the *Rab34*$^{-/-}$ cells and rescued in *Rab34*$^{-/-}$ cells expressing Flag-Rab34. Cilia are marked with arrows, ciliary tubules are marked with arrowheads. Scale bar is 10 microns.

(C) Ift27 (cyan, top) and Ift140 (cyan, bottom) localize to the cilia/centrosomes (red) in WT, *Rab34*$^{-/-}$, and *Rab34*$^{-/-}$ rescue MEF cells.

(D) The percentage of cells able to produce cilia were quantified in serial dilutions of WT and *Rab34*$^{-/-}$ IMCD3 cells. n=>100 cells from 3 independent replicates. Significance was

determined by one-way ANOVA and shown with respect to the same dilution in the other cell line.

(E) GFP-SmoM2 was expressed in WT and *Rab34*$^{-/-}$ IMCD3 cells and subjected to an IN/OUT assay where GFP exposed to the extracellular environment (Out-GFP, red) is labeled prior to permeabilization and staining of total GFP (cyan). The number of internal (left), partially exposed (middle), and exposed (right) cilia were quantified in serial dilutions of WT and *Rab34*$^{-/-}$ IMCD3 cells (bottom). n=>100 cilia from 3 independent replicates except for the lowest density where n=>48. Significance was determined by one-way ANOVA and is shown with respect to the same dilution in the other cell line.

KEY RESOURCES TABLE

REAGENT or RESOURCE	SOURCE	IDENTIFIER
Antibodies		
Flag	Sigma	F1804
Arl13b	Davis/NIH NeuroMab	N295B/66
Arl13b	Proteintech	Arl13b Rabbit PolyAB
Gamma tubulin	Sigma	GTU88
Acetyl-alpha tubulin	Sigma	6–11 B-1
Rab34	Santa Cruz	C-5
Smo	Santa Cruz	E5
Ift27	[4]	719
Ift88	[29]	448
Ift140	[30]	964
Ift25	Proteintech	HSPB11
Streptavidin-488	Invitrogen	S11223
Cep164	Proteintech	Ag17570
Mysoin5a	Novus Biologicals	NBp1–92156
Pacsin-2	Abcam	Ab37615
Rab8	BD Biosciences	610844
GFP	DSHB	DSHB-GFP-12A6
GFP	Invitrogen	3E6
Bacterial and virus strains		
Biological samples		
Chemicals, peptides, and recombinant proteins		
Smoothened Agonist	Calbiochem	566660–1MG
Gibson Assembly Reagent	New England BioLabs	E2611L
Fetal Bovine Serum	Sigma	20C187
DMEM (4.5 glucose/liter)	Sigma	11995–065
Penicillin/Streptomycin	Corning	30–002-Cl
Mercaptoethylamine	Sigma	30070
Glucose oxidase	Sigma	G2133
Catalase	Sigma	C40
Glucose	Sigma	G8270

REAGENT or RESOURCE	SOURCE	IDENTIFIER
NeutrAvidin Resin	Thermo Scientific	29202
Critical commercial assays		
Deposited data		
Experimental models: cell lines		
Wild type MEFs	[2]	11479.6t
Ift27−/− MEFS	[2]	11479.1t
Rab34 −/− MEFs	This study	11479.6t MS34/C22
Wild type IMCD3	[25]	IMCD3
Rab34−/− IMCD3	This study	IMCD3 MS34/C20
Experimental models: organisms/strains		
Oligonucleotides		
GCAATGCATCCTGCACCACCA	Genewiz	MmGAPDHExon3for
TTCCAGAGGGGCCATCCACA	Genewiz	MmGAPDHExon4rev
CTCGACCTGCAAACCGTAATC	Genewiz	MmGli1Exon5for
TCCTAAAGAAGGGCTCATGGTA	Genewiz	MmGli1Exon5/6 junction rev
Recombinant DNA		
Rab34 Guide 1 GGTTGTGGGAGACCTATCTG	This study	MS33
Rab34 Guide 2 GGACAGGTCTTCCCCACAGA	This study	MS34
Cep83 Guide 1 GTCCGAAAACGTTCTCGCAT	This study	MS124
Cep83 Guide 2 ACACCACAAAGCGCTCTTAG	This study	MS125
Sclt1 Guide 1 GAAGCCGATGTACTAAAAAC	This study	MS126
Sclt1 Guide 2 GTGCAGATGATGAGACCGTG	This study	MS127
Cep89 Guide 1 CGCTGGCTTCGGAGCGATGC	This study	MS128
Cep89 Guide 2 GCCCCTCGTTTTCATCCACC	This study	MS129
Cep164 Guide 1 GACCAACGAGGAGGATGAAG	This study	MS130
Cep164 Guide 2 GTACTCAAAGTTACCTCCCA	This study	MS131
Ttbk2 Guide 1 GGTTTTGCAATGAGTGGAGG	This study	MS132
Ttbk2 Guide 2 GGAGAATGTGGCGCTGAAGG	This study	MS133
Ift27-BirA	This study	MS01
Flag-Rab34	This study	MS54

REAGENT or RESOURCE	SOURCE	IDENTIFIER
Rab34 untagged	This study	MS85
Flag-Rab34^{T66N}	This study	MS55
Flag-Rab34^{Q111L}	This study	MS56
Flag-Rab34 $^{C257A/C258A}$	This study	MS57
mCherry-Ripl1	This study	MS134
eGFP-Ccsap	This study	MS122
eGFP-Rab11	This study	MS161
SmoM2-GFP (GFP inserted between SmoM2 codons 32 and 33)	This study	MS198
Software and algorithms		
ImageJ (1.50i (Java 1.8.0_77 [64-bit]))	ImageJ	imagej.nih.gov/ij
GraphPad Prism 8 for Windows 64-bit (version 8.4.3(868))	GraphPad Software, LLC	graphpad.com
Adobe Photoshop CC 2018 (Version: 7 SP1 6.1.7601.24564)	Adobe Inc.	adobe.com
SnapGene	SnapGene Inc	snapgene.com
Scaffold (Version 4.8.8)	Proteome Software	www.proteomesoftware.com
Other		